ELSEVIER

Journal of Power Sources 100 (2001) 93–100

JOURNAL OF POWER SOURCES

www.elsevier.com/locate/jpowsour

Progress in lithium polymer battery R&D

B. Scrosati*, F. Croce, S. Panero

Dipartimento di Chimica, Università di Roma "La Sapienza", 00185 Rome, Italy

Abstract

In this paper the characteristics and performance of composite polymer electrolytes formed by dispersing selected ceramic (e.g. γ-$LiAlO_2$, Al_2O_3, SiO_2) powders in poly(ethylene oxide)–lithium salt (e.g. PEO–$LiCF_3SO_3$) matrices, are reported and discussed. Particular emphasis is devoted to the role of these composite electrolytes in providing the conditions for stabilizing the interface with the lithium metal electrode, as well as for enhancing the electrolyte's overall transport properties. Finally, results based on tests of practical prototypes demonstrate that these unique properties allow the development of new types of high performance, rechargeable lithium polymer batteries.

Keywords: PEO–$LiCF_3SO_3$; Lithium polymer batteries; Solid nanocomposite polymer electrolytes

1. Introduction

Battery technology has achieved spectacular progress in recent years [1]. The most successful product is the rechargeable lithium ion battery that has reached an established commercial status with a production rate of several millions of units per month. However, the success of the lithium ion battery cannot be considered as a point of arrival in the progress of battery technology, since important steps forward can still be achieved by the development of battery systems using lithium metal as the anode. The merit of these systems is the high energy density associated with the high electrochemical factor of the lithium metal electrode. The drawback is the risk associated with the reactivity of this electrode that may affect the cycle life of the battery and ultimately, its safety standards. The safety hazard issue has been controlled in lithium ion technology by using a lithium ion "intercalating" anode, i.e. a compound capable of accepting lithium ions in its lattice and electrons in its electronic structure, e.g. graphite. This "lithium-poor", intercalation anode has been combined with a "lithium-rich", positive intercalation cathode, e.g. lithium cobalt oxide, $LiCoO_2$, in a cell having a lithium ion conducting electrolyte, e.g. a solution of $LiPF_6$ in a solvent mixture of ethylene carbonate–dimethyl carbonate. The electrochemical process of this cell is the cyclic transfer of lithium ions from the lithium-rich positive to the lithium-poor negative [2,3]. Thus, if properly constructed, the cell experiences only a movement of ions without deposition of lithium metal, this greatly reduces the risk of malfunctioning and/or of unexpected side reactions. In addition, the intercalation electrochemistry is characterized by a high reversibility and, in selected cases, by fast kinetics. These favorable properties confer on the lithium ion battery a safe operation combined with a long cycle life and a high rate capability, this finally accounting for its outstanding commercial impact.

As already mentioned, the major problem that prevents the lithium metal battery to achieve a comparable success is the reactivity of the lithium electrode that is corroded in the electrolyte with the formation of a passivation layer on its surface [4]. This non-uniform layer induces irregular lithium deposition upon charge–discharge cycling with the growth of dendrites that eventually may short circuit the cell. A way to face this issue, alternative to the above discussed replacement of the metal with a lithium-intercalating negative, is the replacement of the liquid electrolyte with a liquid-free, lithium ion conducting, membrane. A well known example of these membranes, usually named solid polymer electrolytes, SPEs, is the complex formed by poly(ethylene oxide), PEO and a lithium salt, e.g. $LiCF_3SO_3$ [5–7]. The concept is that of stabilizing the lithium electrode interface by the use of a "dry" solid electrolyte, i.e. by a medium able to prevent any side reactions that may otherwise occur when the metal electrode is in contact with liquid components. In addition, the replacement of the liquid with the polymer electrolyte allows the production of rechargeable lithium polymer batteries, LPBs, that, as a result of their plastic nature, allow flexible, different shape, thin configurations, this being a

* Corresponding author. Tel.: +39-6-491-769; fax:+39-6-446-2866.
E-mail address: scrosati@uniromal.it (B. Scrosati).

0378-7753/01/$ – see front matter
PII: S0378-7753(01)00886-2

feature highly desirable in advanced battery technology [8,9].

All this considered, LPBs are presently viewed as the next generation power sources for the consumer electronic and electric vehicle markets. In particular, it is expected that new types of rechargeable batteries based on a lithium metal anode and a thin film, solvent-free SPE can surpass, in terms of energy density and reliability, the performance of the common lithium ion batteries based on carbonaceous anodes and liquid electrolytes [10]. In principle there are no basic problems that prevent the development of these all-solid LPBs whose large scale production can in fact benefit from the well established fabrication procedures of the polymer industry. In practice, LPB production has so far been hindered by the lack of a suitable polymer electrolyte, i.e. of a membrane separator capable of fulfilling stringent operational requirements in terms of transport properties and of compatibility with the electrode materials. In fact, although in the front line for many years, the PEO-based SPEs have so far not reached a satisfactory status in lithium battery technology due to a series of problems which include: (i) a residual reactivity with the lithium metal electrode, with implications for battery cycle life; (ii) a low lithium ion transference number, with implications for the kinetics of the electrochemical process and thus, for the rate capability of the battery and (iii) an ionic conductivity which becomes adequate only at temperatures above ambient, with implications for the range of utilization of the battery. Large efforts are presently underway to circumvent these remaining issues and in this paper we report the progresses achieved in our laboratory.

2. Optimization of the lithium metal/polymer electrolyte interface

As stressed above, one of the remaining problems to assure a complete successful operation of LPBs is the reactivity of the lithium metal interface. We have demonstrated that this reactivity can be greatly reduced by dispersing selected ceramic powders in the polymer mass, i.e. by producing new types of solid composite PEO-based polymer electrolytes, SCPEs, characterized by enhanced interfacial stability [10]. These SCPEs are typically prepared by hot pressing an intimate mixture of PEO, a lithium salt (e.g. $LiCF_3SO_3$, $LiBF_4$, etc.) and a low particle size ceramic (e.g. γ-$LiAlO_2$, about 4 μm). After cooling in liquid nitrogen, liquid-free, thin, homogeneous and mechanically stable electrolyte membranes are obtained [11].

The stability of the interface between SCPEs and the lithium metal electrode has been controlled by a detailed investigation based on impedance spectroscopy. Indeed, this technique provides a commonly used, effective way to characterize electrode interfaces [12]. In the particular case of the Li electrode/SCPE interface, the study was carried out by monitoring the impedance response of symmetric Li/SCPE/Li cells stored under open circuit condition. Typical results are shown in Fig. 1, which reports the time evolution of the impedance spectra of a cell using PEO–$LiBF_4$–γ-$LiAlO_2$ as the SCPE.

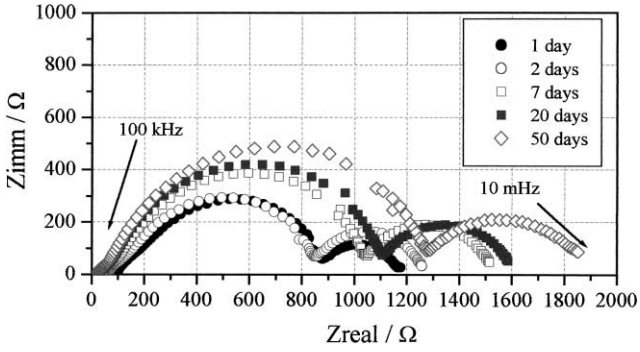

Fig. 1. Impedance response of a Li/$PEO_{20}LiBF_4$ + 20w/o γ-$LiAlO_2$/Li cell at progressive storage times and at 90°C. Frequency range: 10 mHz–100 kHz. Electrode surface: 0.5 cm^2.

One can first notice that the amplitude of the middle-frequency semiarc does not expand consistently with time. Since this amplitude is associated with the overall resistance of the interface, Ri [12], its contained expansion demonstrates that the latter does not grow during storage, this being a preliminary indication of a good stability of the interface. By fitting the evolution of the impedance response reported in Fig. 1 with the help of a proper equivalent circuit [13], one can then refine the analysis to show that the interfacial resistance is in fact the combination of the resistance associated with the passivation film on the lithium electrode surface, R_f; and the resistance associated with charge transfer across the interface, R_{ct}. This is shown in Fig. 2 with reports the time evolution of the two resistance terms.

Clearly, R_f, i.e. the resistance of the electrode surface film resulting from the corrosion reactions that in turn may be responsible for the non-uniform, dendritic deposition of lithium, remains at a very low value over a prolonged length

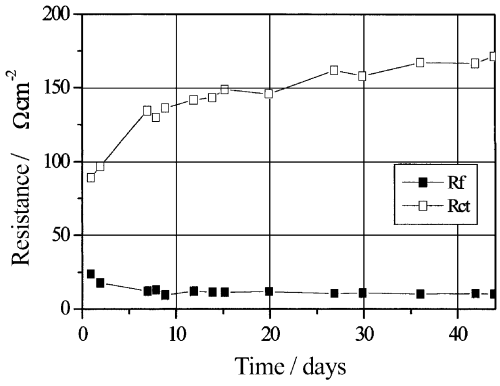

Fig. 2. Charge transfer resistance R_{ct} and passivation layer resistance R_f of the lithium/$PEO_{20}LiBF_4$ + 20w/o γ-$LiAlO_2$ composite polymer electrolyte interface monitored against time at 90°C. Data obtained by impedance spectroscopy.

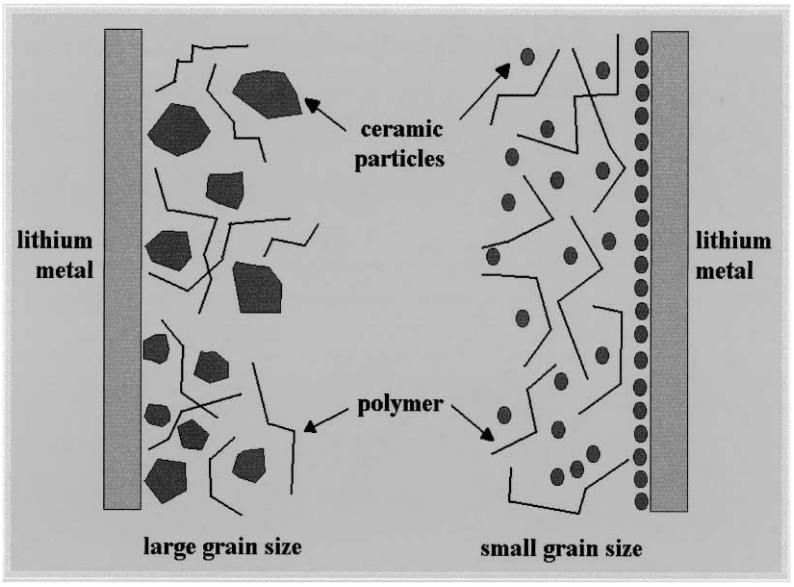

Fig. 3. Schematic model of the lithium electrode/composite electrolyte interface (derived from [14]).

of storage time, this confirming that the Li/SCPE interface may indeed be very stable.

The reason for this improved interfacial stability is associated with the structure and morphology of SCPEs and, in particular to their ''dry'' composition. In fact, the absence of liquid components, i.e. of those elements that are expected to react most easily with the lithium electrode, prevents the growth of the interfacial passivation layer. The stability of the Li/SCPE interface is further enhanced by the dispersed ceramic powders that trap traces of residual liquid impurities and protect the electrode surface, these complementary scavenging and shielding actions being increasingly effective as the particles of the ceramic are reduced in size. Fig. 3 show schematically the model of the Li/SCPE interface [14].

Therefore, one may conclude that it is the ''dry'' composition, combined with the ceramic dispersion, that confers on SCPEs a high interfacial stability to lithium. Accordingly, SCPEs are expected to be suitable media for assuring long cycle life to the lithium electrode. This has been confirmed by monitoring the overvoltage of lithium deposition-stripping cycles in cells using a SCPE separator, a nickel working electrode substrate, a lithium counter electrode and a lithium reference electrode. First, a known amount of charge (deposition charge, Q_D) was passed through the cell in order to promote the deposition of lithium on the nickel substrate. Then, a fraction of this charge (cycling charge, Q_C) was alternately cycled across the cell to promote lithium deposition-stripping cycles and the related overvoltages were monitored upon cycling. The test was assumed to be completed when a significant increase in stripping overvoltage was detected. Fig. 4 shows typical results. The trend of this figure confirms that the lithium deposition-stripping processes extends for more than 700 cycles, this giving a lithium cycling efficiency of the order of 98.6%, i.e. a very high

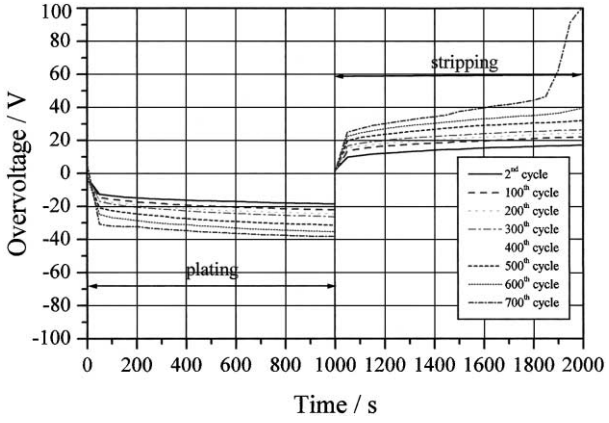

Fig. 4. Lithium plating-stripping overvoltage upon galvanostatic cycling of a lithium metal electrode in a $PEO_{20}LiBF_4 + 20w/o$ γ-$LiAlO_2$ composite polymer electrolyte cell. Ni substrate. $Q_D = 1$ C; $Q_C = 0.1$ C; temperature: 90°C; current density: 0.1 mA cm^{-2}.

value, difficult to achieve with cells based on conventional, ceramic-free, PEO-based electrolytes [15].

3. Conductivity enhancement

Fig. 5 shows the Arrhenius plot of a $PEO_{20}LiBF_4 + 20w/o$ γ-$LiAlO_2$ SCPE. It may be clearly seen that the conductivity curve shows a break around 60–70°C due to the well-known crystalline-amorphous transition of the PEO component [16], this in turn showing that practically useful conductivity values (i.e. in the 10^{-4} S cm^{-1} range) are reached at temperatures higher than ambient and typically around 100°C.

Therefore, although SCPEs have a high interfacial stability, their applicability is still limited by conductivity

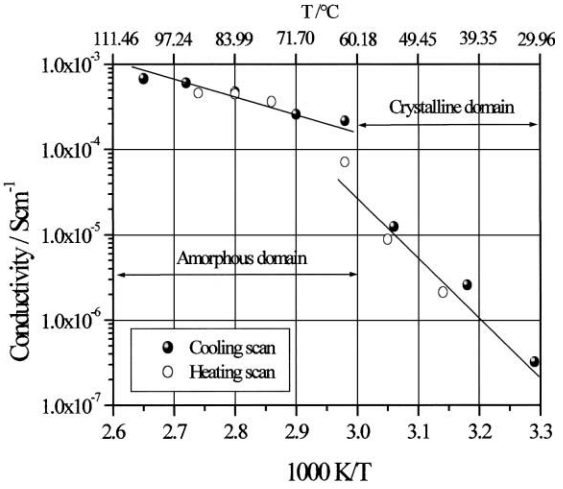

Fig. 5. Arrhenius plots for the $PEO_{20}LiBF_4 + 20w/o\ \gamma\text{-}LiAlO_2$ composite polymer electrolyte sample.

constraints. We have attempted to solve this remaining problem by reducing the particle size of the ceramic fillers to the nanoscale dimension [17]. These new types of PEO-based, nanocomposite polymer electrolytes, SNCPEs, were obtained by first dispersing the selected ceramic powder (e.g. TiO_2, Al_2O_3 or SiO_2) and the lithium salt (e.g. $LiClO_4$, $LiCF_3SO_3$) in acetonitrile and then adding the PEO polymer component. After thorough mixing, the resulting homogeneous slurry was cast between two glass plates provided by spacers to a set thickness, to finally yield mechanically stable membranes of average thickness of about 150 μm.

Fig. 6 shows the conductivity Arrhenius plots of some representative examples of SNCPEs. The as-prepared SNCPEs, e.g. the Al_2O_3-based one, have a room temperature conductivity and a first heating scan similar to those of NCPEs (compare Fig. 5). However, the behavior of the following cooling scan is quite different since no break

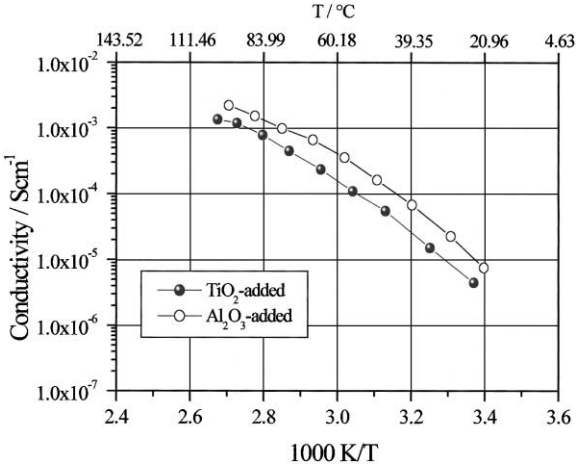

Fig. 6. Arrhenius plots of the conductivity of the nanocomposite PEO_8LiClO_4 10w/o TiO_2, and PEO_8LiClO_4 10w/o Al_2O_3 polymer electrolytes. Data obtained by impedance spectroscopy measurements.

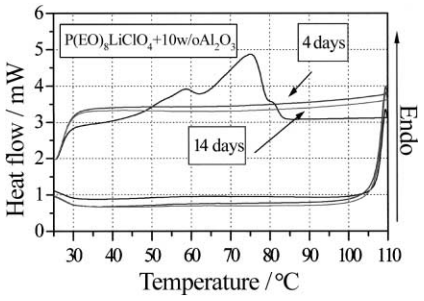

Fig. 7. DSC traces of a PEO–$LiClO_4$ 10w/o Al_2O_3 nanocomposite polymer electrolyte as-prepared and after 4 and 14 days of storage at room temperature. Heating–cooling rate: 10°C min^{-1}.

occurs around 60–70°C and the conductivity remains consistently higher, i.e. between 10^{-3} and 10^{-5} S cm^{-1} (versus 10^{-4} and 10^{-8} S cm^{-1}) in the 80–30°C temperature range. This conductivity trend is reproduced in the following heating and cooling scans.

These results of Fig. 6 are convincing in demonstrating the validity of the nanocomposite approach in enhancing the conductivity of NCPEs. A possible explanation is that, once NCPEs are annealed at temperatures higher than the PEO crystalline to amorphous transition (i.e. above 70°C), the ceramic additive, due to its low particle size and thus, to its large surface area, prevents PEO chain reorganization with the result of freezing at ambient temperature a high degree of disorder which is likely to be accompanied by a consistent enhancement of the ionic conductivity [16].

This model has been confirmed by controlling the crystallization kinetics of the SNCPE samples. Fig. 7 shows the differential scanning calorimetry, DSC, heating–cooling traces of an Al_2O_3-based SNCPE. The heating scan of an as-prepared sample shows a peak around 60–70°C due to the melting of PEO. However, in all the following cooling and heating traces no crystallization peaks are revealed even after prolonged storage times (i.e. exceeding 2 weeks), this demonstrating the acquired amorphous state of the SNCPE.

In addition to stabilizing the amorphous state of the polymer, the dispersed ceramics may promote specific structural modifications via Lewis acid–base reactions between their surface states and the PEO segments. In particular, one may assume that the Lewis acid groups of the ceramics added may quite likely compete with the Lewis acid lithium cations for the formation of complexes with the PEO chains, as well as with the anions of the added LiX salt [18–21]. This in turn may result in local structural modifications occurring at the ceramic surface, due to the specific actions of the polar surface groups of the inorganic filler, which may act as:

1. cross-linking centers for the PEO segments, this lowering the PEO reorganization tendency and thus, promoting a structural modification of the polymer chains; the expected effect is the promotion of Li^+ conducting pathways at the ceramics' surface, this

finally resulting in an enhancement of the ionic conductivity;

2. Lewis acid–base interaction centers for the electrolyte ionic species, this lowering ionic coupling; the expected effect is the promotion of salt dissociation via a sort of ''ion–ceramic complex'' formation, this finally resulting in an enhancement of the lithium ion transference number.

We have undertaken a series of complementary tests to support this model. These have included X-ray [21], impedance spectroscopy [22] and NMR [23] investigations. We have also studied the conductivity and the lithium ion transference number of various SNCPE samples differing in the type and the nature of the ceramic filler. For the latter tests we have selected a PEO–$LiSO_3CF_3$ polymer matrix with the dispersion of 10w/o nanometric Al_2O_3, this ceramic being available in three forms, i.e. acidic, basic and neutral, these in turn reflecting different surface group arrangements [24]. The acidic and neutral forms have a large concentration of surface states, e.g. OH groups, that are expected to favor interactions (via hydrogen bonding) with both the lithium salt anion and the PEO segments, with a consequent expected increase in salt dissociation and in the local PEO amorphous phase fraction. These effects are in turn expected to enhance both the ionic conductivity and the lithium ion transference number, T_{Li}^{+}, of the SNCPE. In contrast, the basic Al_2O_3 form has practically no surface groups, so that no substantial local interactions are foreseen. In summary, the extent of structural modifications induced by the ceramics should be increasing according to the following sequence Al_2O_3 acidic $\approx Al_2O_3$ neutral $>$ Al_2O_3 basic. Fig. 8 shows the Arrhenius conductivity plots of three Al_2O_3-based SNCPE samples and, for comparison purposes also that of a ceramic-free, standard SPE. Indeed, the trends of this figure confirm that while the conductivity

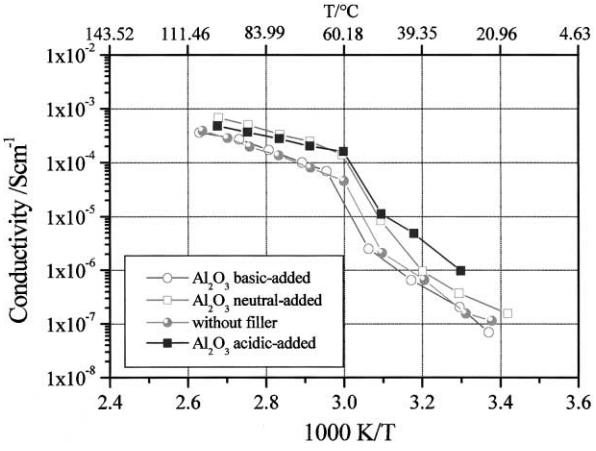

Fig. 8. Conductivity Arrhenius plots of PEO–$LiCF_3SO_3$ nanocomposite polymer electrolytes with the addition of 10w/o Al_2O_3 in its acid, neutral and basic form, respectively. The Arrhenius plot of a ceramic-free, PEO–$LiCF_3SO_3$ electrolyte is also reported for comparison purposes. Data obtained from impedance spectroscopy.

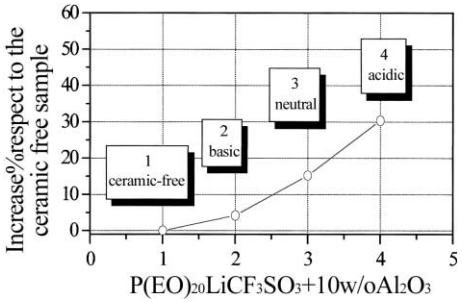

Fig. 9. Percentage changes in lithium transference number in a ceramic-free, PEO–$LiCF_3SO_3$ electrolyte and in PEO–$LiCF_3SO_3$ nanocomposite polymer electrolytes formed with the addition of 10w/o Al_2O_3 in its acid, neutral and basic form, respectively.

of the composites based on acidic and neutral, Al_2O_3 filler, respectively, is higher than that of the corresponding ceramic-free sample, no substantial differences are noticed for the Al_2O_3 basic added composite, this being consistent with the model above discussed.

The local surface interaction model has been further supported by evaluation the Li^+ transference number T_{Li}^{+}, of the four samples, i.e. the Al_2O_3 acidic, basic and neutral, respectively, composites and, again for comparison purposes, that of a ceramic-free sample. The T_{Li}^{+} parameter was determined by imposing ac and dc polarization pulses, on cells of the Li/electrolyte sample/Li type and by following the time evolution of the resulting current flow [25]. To improve the accuracy of the results, we have developed a special software capable of acquiring a very large number of values of the current flowing immediately after the application of the voltage pulse.

Fig. 9, which reports the results in terms of percentage of changes of T_{Li}^{+}, confirms the specific role of the surface groups of the filler by showing a progressive increase in T_{Li}^{+} when passing from the ceramic-free to the three composites having in turn, basic, neutral and acidic Al_2O_3 dispersion. On the basis of the above discussed results one may conclude that in the SNCPEs the role of the filler is not limited to the sole action of preventing crystallization of the polymer chains but also, and in particular, of promoting specific interactions between the surface groups and both the PEO segments and the electrolyte ionic species. These locally induced structural modifications result in the increase of the fraction of ''free'' Li^+ ions which can move fast throughout the conducting pathways at the ceramic extended surface. These modifications result in enhancements in the ionic conductivity over a wide temperature range, as well as in the Li^+ ion transference number. It is be noted that these properties are particularly important in view of applications in practical lithium batteries. The enhancement in conductivity is beneficial in terms of internal resistance. The enhancement in Li^+ ion transference number is beneficial in terms of the discharge kinetics. In fact, LPBs are most commonly based on an electrochemical process that is the insertion–extraction of the Li^+ ions in and from selected

intercalation cathodes [7]. Under these conditions, the cell operation is solely controlled by the transport of the Li^+ ions throughout the electrolyte, so that a high transference number results in low concentration polarization, this in turn allowing high discharge rates. Other bonuses of SNCPEs are the excellent mechanical properties associated with the liquid-free, solid configuration and further reinforced by the ceramic network. In view of all these favorable properties, that have also been confirmed by other authors [26,27], the SNCPEs are expected to behave as superior separators for high performance LPBs.

4. Relevance of SNCPEs for practical battery applications

It has appeared to us of importance to assemble prototypes of LPBs in order to ascertain the validity of the above considerations. The system formed by dispersing nanoparticle size, ''neutral'' Al_2O_3 in a PEO–$LiCF_3SO_3$ matrix was chosen as the preferred SNCPE. As in the general case of PEO-based batteries, the choice of the cathode active material was somewhat restricted by the thermodynamic stability of the SNCPE which does not exceed 4 V versus Li [28]. This excludes common high voltage cathodes, such as $LiCoO_2$ and $LiMn_2O_4$, and limits the choice to those cathodes that are able to undergo the complete electrochemical process (in terms of battery totally acquiring/releasing the charge) at potentials around 3.5 V versus Li. Very few cathode materials are known to accomplish this requirement but among them, the $LiFePO_4$ of the phospho-olivine family proposed by Goodenough and co-workers [29] and the $LiMn_3O_6$ spinel studied by Xia et al. [30] appeared particularly suitable to be used in connection with our improved SNCPEs.

The Li/SNCPE/$LiFePO_4$ battery [31] and the Li/SNCPE/$LiMn_3O_6$ battery [32] prototypes were assembled by sandwiching the SNCPE film between a lithium metal foil anode backed on to a copper foil current collector and a cathode film formed by casting on an aluminum current collector a slurry of the active material ($LiFePO_4$ or $LiMn_3O_6$) mixed with a carbon conductive additive and a PVdF (Solvay Solef 6020, 3 wt.%) binder.

Fig. 10 shows typical charge–discharge cycles at 105°C of the Li/SNCPE/$LiFePO_4$ battery [31]. The result indeed confirms that the battery offers unique and excellent behavior. The voltage evolves with a peculiarly flat profile around 3.5 V, i.e. well below the decomposition limit of PEO systems. The overall electrochemical process, that involves the reversible extraction of Li^+ ions from $LiFePO_4$ with the formation of $FePO_4$ [29]

$$LiFePO_4 \Leftrightarrow FePO_4 + Li^+ + 1e^- \quad (1)$$

proceeds with the exchange of about 0.8 mol of Li for cathode formula unit, corresponding to a specific capacity of 135 mAh g^{-1}. The striking structural similarities of the two solid phases accounts for the flatness of the charge–discharge voltage profiles. Thus, the favorable behavior of the $LiFePO_4$ cathode, already shown by Goodenough and co-workers in liquid electrolytes [29] and by Armand and co-workers in conventional, ceramic-free polymer electrolytes [33], is here confirmed. However, it is the combination of this cathode material with our SNCPBs which leads to new lithium polymer battery systems with unique features in terms of cycle life and of power capability. This is due to the above stressed lithium interfacial stabilization provided by the ceramic filler that assures a high reversibility of the lithium deposition-stripping process, this in turn greatly contributing to assure a prolonged cycling for the battery. Indeed, this is well demonstrated by the results reported in Fig. 11 which show over 250 charge–discharge cycles with very limited decay in capacity.

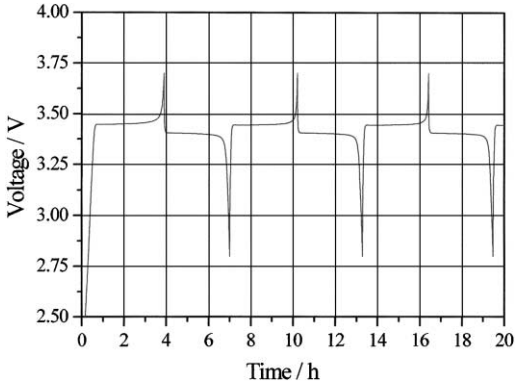

Fig. 10. Charge–discharge galvanostatic cycles of the Li/$(PEO)_{20}$ $LiCF_3SO_3$ + 10w/w Al_2O_3/$LiFePO_4$ battery at 105°C and at *C*/3 rate.

In addition, due to the enhancement in lithium ion transference number in the electrolyte promoted by the dispersion of the ceramics, the battery can operate at unusually high power rates. This is confirmed by the same Fig. 11 which shows that the battery cycles well at 1 C and by Fig. 12 which demonstrates that the same battery can sustain current rates up to about 2 C before reaching diffusion controlled

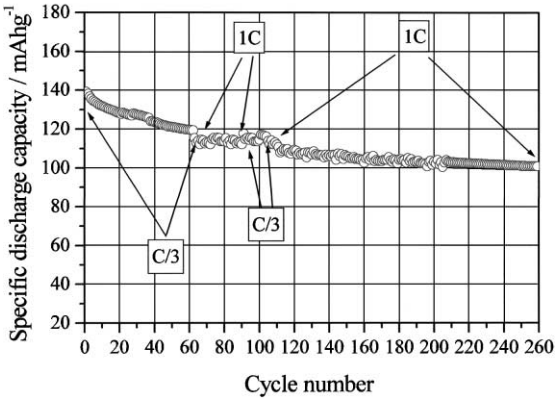

Fig. 11. Cycleability of the Li/$(PEO)_{20}LiCF_3SO_3$ + 10w/w Al_2O_3/$LiFePO_4$ battery at 105°C.

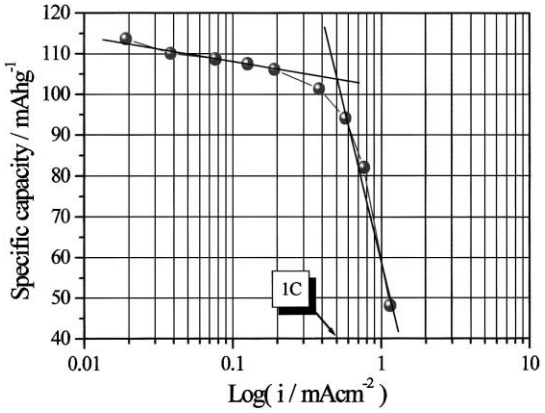

Fig. 12. Polarization curve of the Li/$(PEO)_{20}LiCF_3SO_3$ + 10w/w Al_2O_3/$LiFePO_4$ battery at 105°C.

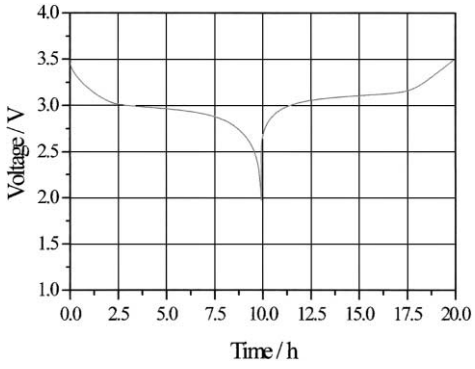

Fig. 13. Typical charge–discharge curve of the Li/$(PEO)_{20}LiCF_3SO_3$ + 10w/o Al_2O_3/$LiMn_3O_6$ polymer cell at 70°C and at *C*/10 (43 μA cm^{-2}).

kinetics determined by concentration, polarization. It is important to point out that the current density levels associated with these high rates are far beyond the limiting values reported in the literature for conventional Li polymer batteries [34]. This difference is clearly associated with the difference in the value of the lithium ion transference number which passes from 0.2 to 0.3 in conventional ceramic-free polymer electrolytes to 0.5–0.6 in the nanocomposites (see Fig. 9).

In addition to improving transference number, the dispersion of ceramic fillers also enhances the ionic conductivity, so that SNCPEs are expected to allow LPB operation at lower temperatures than the 100°C range typically needed for running batteries based on common ceramic-free SPEs [34]. To confirm this expectation, we have tested the response of a LPB using again $(PEO)_{20}LiCF_3SO_3$ + 10w/w Al_2O_3 as the SNCPE separator and $LiMn_3O_6$ as the selected cathode [32]. Similarly to $LiFePO_4$, $LiMn_3O_6$ offers interesting properties as a cathode material for rechargeable LPBs. In fact, $LiMn_3O_6$ also operates in the 3 V range, i.e. within the stability window of the PEO-based polymer electrolytes, and offers a high capacity, i.e. of the order 210 mAh g^{-1}, corresponding to 0.67 Li^+ per mol intercalation, according to the following electrochemical process:

$$LiMn_3O_6 + 2Li^+ + 2e^- \Leftrightarrow 3LiMnO_2 \quad (2)$$

In addition, manganese oxides are inexpensive and non-toxic, this being a further bonus for use in LPBs, especially in view of the application of these batteries in electric vehicles.

Fig. 13 shows a typical discharge curve of the Li/$LiMn_3O_6$ cell at the *C*/10 rate and at 70°C, i.e. at a temperature substantially lower than that usually adopted for common LPBs. The discharge capacity is of the order of 170 mAh g^{-1} referred to the $LiMn_3O_6$ cathode, this showing that the battery operates with the exchange of 0.54 Li^+ per mol (see reaction [2,3]), i.e. at about 80% of the maximum theoretical capacity.

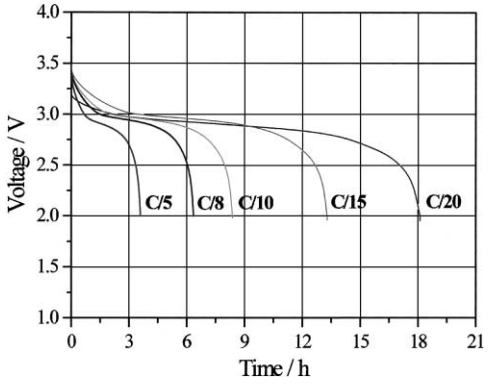

Fig. 14. Discharge curves of the Li/$(PEO)_{20}LiCF_3SO_3$ + 10w/o Al_2O_3/$LiMn_3O_6$ polymer cell at various discharge rates and at 70°C. Charge rate: *C*/10.

The power capabilities of the battery are demonstrated by Fig. 14 which shows discharge curves at various rates from *C*/20 to *C*/5 and by Fig. 15 which shows the capacity delivery upon cycling at different rates. The results confirm that even at the moderate temperature of operation, the battery can sustain high current rates before reaching controlled

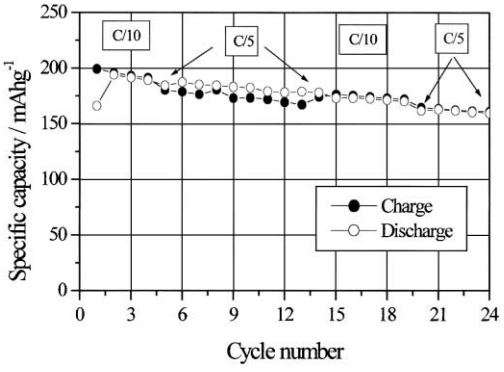

Fig. 15. Capacity delivery upon cycling of the Li/$(PEO)_{20}LiCF_3SO_3$ + 10w/o Al_2O_3/$LiMn_3O_6$ polymer cell at 70°C at various discharge rates. Voltage limits: 3.5–2.0 V.

kinetics determined by concentration polarization. In addition, the battery has an excellent cycle life, showing a low degree of capacity loss over a great number of high rate cycles. All these features are well beyond the limiting values achievable for conventional LPBs at 70°C, this finally establishing the key role of the SNCPEs in assuring the development of new types of high performance LPBs.

5. Conclusion

The results reported in this work show that SNCPEs may indeed be exploited for the development of LPBs characterized by unique features. In fact, the high interfacial stability of SNCPEs allows long cycle life and their improved transport properties allow low temperature operation as well as high discharge rates. These features have been demonstrated by illustrating the response of two new types of LPBs, based on $(PEO)_{20}LiCF_3SO_3 + 10w/o\ Al_2O_3$ as preferred SNCPE and on a phospho-olivine $LiFePO_4$ and a spinel $LiMn_3O_6$, respectively, as the cathode. Both batteries are capable of operating under discharge currents higher and temperature ranges lower than those usually achievable with conventional LPBs. The practical relevance of these new types of rechargeable LPBs is further substantiated by their energetic content. In fact, evaluations based on the average cathode capacity and voltage, give for the $Li/SNCPE/LiFePO_4$ battery a theoretical energy density of 477 Wh kg^{-1} and for the $Li/SNCPE/LiMn_2O_3$ battery a theoretical energy density of 500 Wh kg^{-1}, both values being comparable to the 475 Wh kg^{-1} associated with the Li/V_6O_{13} electrodic couple currently used for the development of the most promising Li polymer batteries so far [34].

Acknowledgements

This work was carried out with the financial support of the US Army European Research Office, Contract No. 68171-00-M-5848. The authors wish to thank the Chunco Denki Koygo Co. Ltd., Japan, for kindly providing the $LiMn_3O_6$ cathode samples. Thanks are also expressed to Dr. G.B. Appetecchi, L. Persi and F. Ronci for the experimental work.

References

[1] B. Scrosati, Nature 373 (1995) 557.
[2] S. Megahed, B. Scrosati, J. Power Sources 51 (1994) 79.
[3] S. Megahed, B. Scrosati, Interface 4 (4) (1995) 34.
[4] E. Peled, in: J. Gabano (Ed.), Lithium Batteries, Academic Press, New York, 1983, pp. 43–69.
[5] M. Armand, Faraday Discuss. Chem. Soc. 88 (1989).
[6] C.A. Vincent, Chemistry in Britain, 1989, p. 391.
[7] B. Scrosati, in: C.A. Vincent, B. Scrosati (Eds.), Modern Batteries, Arnold, London, 1997, pp. 198–240.
[8] B. Scrosati, Chem. Rec. 1 (2001) 173.
[9] C.A. Vincent, B. Scrosati, Bull. Mat. Soc. Bull. Mat. Res. Soc. 25 (2000) 28.
[10] M.C. Borghini, M. Mastragostino, S. Passerini, B. Scrosati, J. Electrochem. Soc. 142 (1995) 2118.
[11] G.B. Appetecchi, F. Croce, G. Dautzenberg, M. Mastragostino, F. Ronci, B. Scrosati, F. Soavi, F. Zanelli, F. Alessandrini, P.P. Prosini, J. Electrochem. Soc. 145 (1998) 4126.
[12] J. Ross Macdonald, Impedance Spectroscopy, Wiley, New York, 1987.
[13] B.A. Boukamp, Solid State Ionics 20 (1986) 159.
[14] F. Gray, M. Armand, Polymer electrolytes, in: T. Osaka, M. Datta (Eds.), Energy Storage Systems for Electronics, Gordon and Breach, Australia, 2000, pp. 351–406.
[15] G.B. Appetecchi, F. Croce, L. Persi, F. Ronci, B. Scrosati, Electrochim. Acta 45 (2000) 1481.
[16] F.M. Gray, Polymer Electrolytes, Royal Society of Chemistry Monographs, Cambridge, 1997.
[17] F. Croce, G.B. Appetecchi, L. Persi, B. Scrosati, Nature 394 (1998) 456.
[18] B. Kumar, L.G. Scanlon, J. Power Sources 52 (1994) 261.
[19] W. Wieczorek, Z. Florjancyk, J.R. Stevens, Electrochim. Acta 40 (1995) 2251.
[20] J. Przyluski, M. Siekierski, W. Wieczorek, Electrochim. Acta 40 (1995) 2101.
[21] F. Croce, R. Curini, A. Martinelli, L. Persi, F. Ronci, B. Scrosati, R. Caminiti, J. Phys. Chem. B103 (1999) 10632.
[22] B. Scrosati, F. Croce, L. Persi, J. Electrochem. Soc. 147 (2000) 1718.
[23] S. Greenbaum, S. Chung, Y. Wang, L. Persi, F. Croce, B. Scrosati, J. Power Sources, in press.
[24] F. Croce, L. Persi, B. Scrosati, F. Serraino-Fiory, E. Plichta, M.A. Hendrickson, Electrochim. Acta 46 (2001) 2457.
[25] J. Evans, C.A. Vincent, P.G. Bruce, Polymer 28 (1987) 2325.
[26] A.S. Best, J. Adebahr, P. Jacobsson, D.R. MacFarlane, M. Forsyth, in press.
[27] P. Capiglia, P. Mustarelli, E. Quartarone, C. Tomasi, A. Magistris, Solid State Ionics 118 (1999) 73.
[28] Y. Xia, T. Fujieda, K. Tatsumi, P.P. Prosini, T. Sakai, J. Power Sources 92 (2000) 234.
[29] A.K. Padhi, K.S. Nanjundaswamy, J.B. Goodenough, J. Electrochem. Soc. 144 (1997) 1188.
[30] Y. Xia, K. Tatsumi, T. Fujieda, P.P. Prosini, T. Sakai, J. Electrochem. Soc. 147 (2000) 2050.
[31] F. Croce, F. Serraino-Fiory, L. Persi, B. Scrosati, Electrochem. Solid State Lett. 4 (2001) A121.
[32] L. Persi, B. Scrosati, E. Plichta, M.A. Hendrickson, J. Electrochem. Soc., submitted for publication.
[33] N. Ravet, J.B. Goodenough, S. Besner, M. Simoneau, P. Hovignon, M. Armand, in: Proceedings of the 196th ECS Meeting on Improved Iron-Based Cathode Material, Hawaii, 17–22 October, Abstract 127, 1999.
[34] P.P. Prosini, S. Passerini, R. Vellone, W.H. Smyrl, J. Power Sources 75 (1998) 73.